

# Mechanistic Insights into a Gas–Solid Reaction in Molecular Crystals: The Role of Hydrogen Bonding\*\*

Guillermo Mínguez Espallargas, Jacco van de Streek, Philippe Fernandes, Alastair J. Florence, Michela Brunelli, Kenneth Shankland, and Lee Brammer\*

Reactions in (molecular) organic crystalline solids have been shown to be important for exerting control that is unattainable over chemical transformations in solution.<sup>[1–3]</sup> Such control has also been achieved for reactions within metal–organic cages.<sup>[4]</sup> In these examples, the reactants are already in place within the crystals following the original crystal growth. The post-synthetic modification of metal–organic frameworks (MOFs)<sup>[5,6a,b]</sup> and indeed reactions and catalysis within MOFs<sup>[5b,c,6]</sup> have been recently demonstrated; in these cases the reactants enter the crystals through permanent channels. Another growing area of interest within molecular solid-state chemistry is synthesis by mechanical co-grinding of solid reactants—often referred to as mechanochemistry.<sup>[7,8]</sup> Finally, in a small number of reported examples, molecules also have been shown to enter nonporous crystals directly from the gas or vapor phase,<sup>[9–11]</sup> but in only a few of these examples does a change in covalent bonding result, which indicates that a reaction occurs within the nonporous crystals.<sup>[10,11]</sup> It is this latter type of highly uncommon reaction that is the focus of the present study.

Collectively, these classes of reactions, which involve what may be loosely termed the “molecular solid state” that encompasses coordination polymers and metal–organic frameworks,<sup>[12]</sup> have contributed to the growth of what is clearly becoming a hugely important new area of materials

synthesis.<sup>[13]</sup> However, in stark contrast to well-established solution-phase syntheses, mechanistic information on molecular-solid-state reactions is at present extremely limited,<sup>[14]</sup> and is entirely absent in most cases. This lack of information reflects not only the infancy of the field of reactions and synthesis in the molecular solid state, but also the challenges faced in either the experimental determination or computational modeling of reaction (and transport) mechanisms.

We provide herein a mechanistic insight into a reaction that takes place in a crystalline molecular solid. We describe the reaction of HCl gas with nonporous molecular crystals of *trans*-[CuBr<sub>2</sub>(3-Brpy)<sub>2</sub>] **1** (3-Brpy = 3-bromopyridine) to give the crystalline product (3-BrpyH)<sub>2</sub>[CuBr<sub>2</sub>Cl<sub>2</sub>] **2**. The reaction involves cleavage of Cu–N and H–Cl bonds and formation of new Cu–Cl and N–H bonds. The product has been structurally characterized by X-ray powder diffraction, wherein Rietveld refinement has enabled distinction to be made between chloride and bromide sites (X) of the anion. The nonrandom distribution of halide sites observed provides the mechanistic insight and, specifically, points to the directing role of hydrogen-bonding interactions (and to a lesser extent the halogen-bonding interactions) that are formed in the product.

A sample of **1** was prepared in quantitative yield as a green microcrystalline solid by direct reaction of CuBr<sub>2</sub> with 3-bromopyridine in MeOH. The crystal structure of **1** was determined from experimental X-ray powder diffraction data using simulated annealing methods followed by Rietveld refinement and confirms that **1** is isostructural with the previously reported *trans*-[CuCl<sub>2</sub>(3-X'py)<sub>2</sub>] compounds (X' = Cl, Br).<sup>[11a]</sup> The crystal structure of **1** contains molecules of *trans*-[CuBr<sub>2</sub>(3-Brpy)<sub>2</sub>], in which the Cu<sup>II</sup> centers adopt a square-planar coordination geometry. The molecules interact through well-defined C–Br⋯Br–Cu halogen bonds between the bromopyridyl and bromide ligands of neighboring molecules.<sup>[15]</sup> These interactions involve all bromine atoms. Previously, we have shown that microcrystalline *trans*-[CuCl<sub>2</sub>(3-Clpy)<sub>2</sub>] and *trans*-[CuCl<sub>2</sub>(3-Brpy)<sub>2</sub>] react directly with either dry HCl gas or vapors from concentrated aqueous HCl to give the salts (3-ClpyH)<sub>2</sub>[CuCl<sub>4</sub>] and (3-BrpyH)<sub>2</sub>[CuCl<sub>4</sub>], respectively, as crystalline products.<sup>[11a,b]</sup> However, without isotopically labeling the chlorine atoms, it is not possible to extract mechanistic information since the chloride ligands in the reactants are indistinguishable from those in the products.

In the present study, we sought to overcome this problem by making use of the similarity in size and chemical behavior of Cl and Br to effect a labeling experiment. Thus, in separate experiments, **1** was exposed to dry HCl gas (3 days) or to

[\*] Dr. G. Mínguez Espallargas,<sup>[†]</sup> Prof. L. Brammer  
Department of Chemistry, University of Sheffield  
Sheffield S3 7HF (UK)  
Fax: (+44) 114-222-9346  
E-mail: lee.brammer@sheffield.ac.uk  
Homepage: <http://www.shef.ac.uk/chemistry/staff/profiles/brammer.html>

Dr. J. van de Streek  
Avant-garde Materials Simulation  
Merzhauserstr. 177, 79100 Freiburg (Germany)

Dr. P. Fernandes, Prof. A. J. Florence  
Strathclyde Institute of Pharmacy and Biomedical Sciences  
University of Strathclyde (Scotland)

Dr. M. Brunelli  
European Synchrotron Radiation Facility, 38042 Grenoble (France)

Dr. K. Shankland  
School of Pharmacy, University of Reading (UK)

[†] Current address: Instituto de Ciencia Molecular (ICMol)  
Universidad de Valencia, Paterna (Spain)

[\*\*] We thank the CCDC and STFC Centre for Molecular Structure & Dynamics (GME) for financial support and the ESRF for access to beam line ID31.

Supporting information for this article is available on the WWW under <http://dx.doi.org/10.1002/anie.201003265>.

vapor from concentrated aqueous HCl (4 days). A color change of the solid from green to brown was observed in each case (Figure 1).

The crystallinity of the product was established and its phase purity examined by X-ray powder diffraction for both

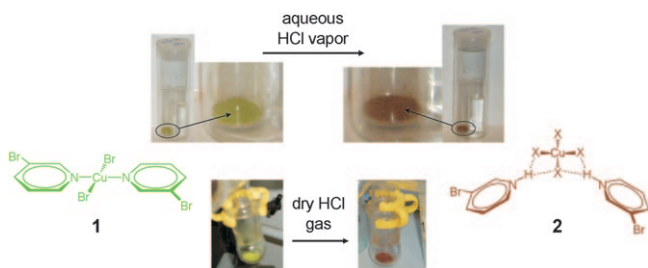


**Figure 1.** Reaction of green microcrystalline  $\text{trans-[CuBr}_2\text{(3-Brpy)}_2\text{]} \mathbf{1}$  with HCl to yield brown microcrystalline  $\text{(3-BrpyH)}_2\text{[CuX}_4\text{]} \mathbf{2}$  ( $\text{X} = \text{Cl}$  and/or Br).

reactions with HCl. The results indicate close to quantitative conversion to a material that is isostructural with the salt  $\text{(3-BrpyH)}_2\text{[CuCl}_4\text{]}$ . Rietveld refinement was undertaken for both products, starting from a structural model derived from the crystal structure of  $\text{(3-BrpyH)}_2\text{[CuCl}_4\text{]}$  by replacing the four chloride ligands by atomic sites each with a chloride/bromide population ratio of 50:50 (Figure 2). The total population for each site was constrained to unity during structure refinement, but the Cl/Br ratio was allowed to refine and Cl and Br positions were not constrained to be identical. The products of both reactions consistently showed a composition that was in agreement with the formula  $\text{(3-BrpyH)}_2\text{[CuBr}_2\text{Cl}_2\text{]} \mathbf{2}$ ,<sup>[16]</sup> thus indicating the addition of two equivalents of HCl per molecule of **1**. This determination is significant since it indicates that Br is not lost during the reaction and that therefore most probably the original bromide sites are not replaced by chloride. Most significant,

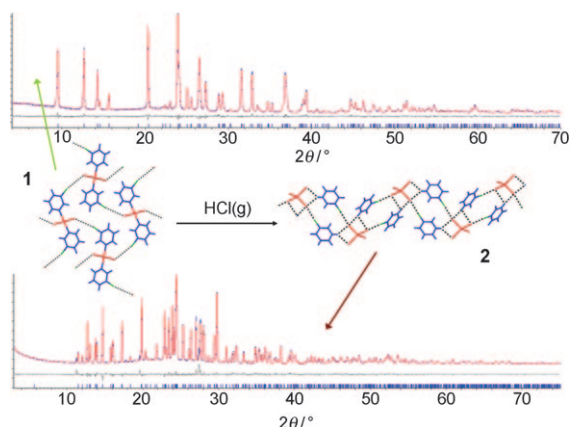


**Figure 2.** Crystal structures of **1** and **2**. Copper atoms and halide ligands are shown in red, bromine substituents in green, and pyridyl/pyridinium rings in blue. Dotted lines represent  $\text{N-H}\cdots\text{X-Cu}$  hydrogen bonds and  $\text{C-Br}\cdots\text{X-Cu}$  halogen bonds. Observed (blue) and calculated (red) profiles and difference plot ( $I_{\text{obs}} - I_{\text{calc}}$ ; gray) of the Rietveld refinement of compounds **1** (top;  $2\theta$  range  $4.0\text{--}70.0^\circ$ ; max. resolution  $1.34 \text{ \AA}$ ) and **2a** (bottom;  $2\theta$  range  $4.0\text{--}75.0^\circ$ ; max. resolution  $1.27 \text{ \AA}$ ).

however, is that the distribution of the halide sites within the anions is not random. Furthermore, the atomic populations at each of the four halide sites are consistent between the products of reaction with aqueous HCl vapor (**2a**) and reaction with dry HCl gas (**2b**). Specifically, one of the four sites is rich in chloride (ca. 67:33 Cl/Br) and one is highly deficient (ca. 17:83 Cl/Br), whereas the other two sites have slightly elevated chloride populations (Cl 55–62%; Br 45–38%; Figure 3).

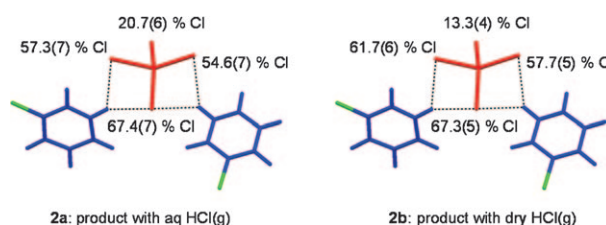
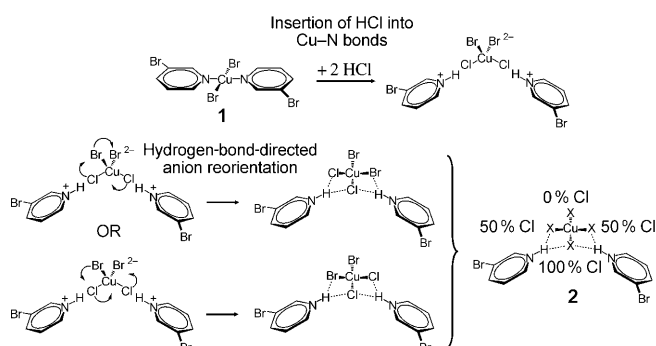


**Figure 3.** Experimentally determined occupancies for Cl at the halide ligand sites in **2**. Percentage occupancies for Br can be calculated by ( $\% \text{Br} = 100 - \% \text{Cl}$ ).  $\text{N-H}\cdots\text{X-Cu}$  hydrogen bonding between cations and anions is shown as dotted lines.  $\text{C-Br}\cdots\text{X-Cu}$  halogen bonding (not shown) is also present in the crystals at the two halide sites with highest Cl occupancy. See Figure 2 for color codes.

These structure determinations provide important insight into the mechanism of the reaction between crystalline **1** and gaseous HCl. Specifically, the Cl/Br distribution found in the anions implicates a mechanism in which insertion of HCl into the  $\text{Cu-N}$  bonds of **1** to give  $\text{(3-BrpyH)}_2\text{[CuBr}_2\text{Cl}_2\text{]}$  is followed by reorientation of the anions to result in the structurally observed distribution of chloride and bromide ligands found in **2** (Scheme 1). This distribution can be rationalized based upon the relative strengths of intermolecular interactions involving chloride and bromide ligands, thus competition exists between  $\text{N-H}\cdots\text{Cl-Cu}$  and  $\text{N-H}\cdots\text{Br-Cu}$  hydrogen bonds, and between  $\text{C-Br}\cdots\text{Cl-Cu}$  and  $\text{C-Br}\cdots\text{Br-Cu}$  halogen bonds. Both types of interaction are strongly electrostatically driven and in both cases the interaction formed with the chloride ligand will be stronger because of its greater accumulation of negative charge and therefore more negative electrostatic potential.<sup>[17,18]</sup>



**Scheme 1.** Sequential steps in the mechanism of the gas-solid reaction between HCl and **1**, emphasizing the enthalpic influence of hydrogen bonding on the anion orientation. The two halide sites shown as equivalent in this model can be further distinguished by accounting for halogen-bond formation (not shown).

Three of the four halide sites in the anions are involved in hydrogen bonding to the 3-bromopyridinium ions: one site is involved in two bifurcated hydrogen bonds and two sites participate in one part of a bifurcated hydrogen bond (Figure 3). Greater participation in hydrogen bonding correlates with increased Cl population at that site, or considering individual  $[\text{CuBr}_2\text{Cl}_2]^{2-}$  ions in the structure, a larger proportion adopt orientations that place chloride ligands in the sites with greater involvement in hydrogen bonding.<sup>[19]</sup> Thus, it can be argued that there is an enthalpic driving force for a halide site distribution that is approximated by the average of the two products of anion reorientation shown in Scheme 1, suggesting Cl populations of 100, 50, 50, and 0%. However, entropic forces would favor a random distribution that leads to 50% of each halide at each site. The observed distribution should result from minimizing the free energy, which accounts for these two competing influences. Based upon consideration only of hydrogen bonding, a “symmetric” distribution of halide sites would be anticipated in which there is one site with the highest Cl content, two sites with a lower but equal Cl content, and one site with the lowest Cl content. However, two of the halide sites also serve as halogen-bond acceptors that form  $\text{C}-\text{Br}\cdots\text{X}-\text{Cu}$  halogen bonds involving neighboring cations (Figure 2). Such interactions are also expected to be enthalpically favored on electrostatic grounds for  $\text{X} = \text{Cl}$  over  $\text{X} = \text{Br}$ .<sup>[18]</sup> Accordingly, the two sites involved in halogen bonds have the highest Cl populations of approximately 67 and 57–62% and indeed the rank order of the four sites in terms of Cl population correlates with the total number of strong intermolecular interactions formed, either hydrogen bond or halogen bond (Table 1).

**Table 1:** Relationship between intermolecular interactions at the anion and the Cl/Br ratio at the halide sites.

Halide site <sup>[a]</sup>	Cl %	Br %	No. of hydrogen bonds (HB)	No. of halogen bonds (XB)	HB + XB
1	67.4(7) [2a]	32.6(7) [2a];	2	1	3
	67.3(5) [2b]	32.7(5) [2b]			
2	57.3(7) [2a];	42.7(7) [2a];	1	1	2
	61.7(6) [2b]	38.3(6) [2b]			
3	54.6(7) [2a];	45.4(7) [2a];	1	0	1
	57.7(5) [2b]	42.3(5) [2b]			
4	20.7(6) [2a];	79.3(6) [2a];	0	0	0
	13.3(4) [2b]	86.7(4) [2b]			

[a] Rank order by Cl occupancy.

We have previously established that the related reaction between *trans*- $[\text{CuCl}_2(3\text{-Clpy})_2]$  and HCl to produce  $(3\text{-ClpyH})_2[\text{CuCl}_4]$  is a gas–solid equilibrium reaction.<sup>[11b]</sup> It is reasonable to assume that the reaction of **1** with HCl gas proceeds in an analogous manner given the isostructural relationship between reactants **1** and *trans*- $[\text{CuCl}_2(3\text{-Clpy})_2]$ , and between products **2** and  $(3\text{-ClpyH})_2[\text{CuCl}_4]$ . Thus, given this equilibrium behavior, it is instructive to consider the implication that the product **2** is formulated as containing  $[\text{CuBr}_2\text{Cl}_2]^{2-}$  ions. This formulation indicates that under the reaction conditions used (or over the reaction period studied),

only HCl gas is released, rather than a mixture of HCl and HBr, in the reverse reaction that contributes to the equilibrium. Possible thermodynamic (enthalpic) explanations for this somewhat unexpected conclusion are that Cu–Br bonds are stronger than Cu–Cl bonds in the bond-breaking contribution, or that H–Br bonds are weaker than H–Cl bonds in the bond-forming step. Although the latter assertion is consistent with the observed behavior, the former is not consistent, as Cu–Br bonds are expected to be weaker than Cu–Cl bonds.<sup>[20]</sup> A simpler explanation based on a kinetic argument could be that the larger HBr molecule cannot escape the crystals as readily as HCl. Such a possibility is under further investigation.

There is no doubt that mechanistic information will be of great value in fully developing and exploiting the synthesis of new crystalline molecular materials. The great challenge will be designing, and even developing experimental techniques to extract mechanistic information. The present study was designed to probe the mechanism through recognition that the behavior of Cl and Br is sufficiently similar that the product  $(3\text{-BrpyH})_2[\text{CuX}_4]$  could be anticipated based upon our earlier studies on reactions of *trans*- $[\text{CuCl}_2(3\text{-Clpy})_2]$  and *trans*- $[\text{CuCl}_2(3\text{-Brpy})_2]$  with HCl gas. However, since Cl and Br exhibit sufficiently different X-ray scattering power, high-quality powder X-ray diffraction data can be used to detect the presence of each anion, even when populating a common site in the crystal structure. In effect, this can be considered as a type of labeling experiment, which is a common approach in investigating mechanisms of solution-phase reactions, although isotopic labeling is more common. The structural information established herein has enabled us to postulate a mechanism in which insertion of HCl into the Cu–N bonds of **1** is followed by reorientation of the anions in the product **2**. The reorientation is driven by formation of the strongest hydrogen bonds and supported by maximizing stronger halogen-bond formation, in both cases by increasing the preference for chloride over bromide at the sites of such intermolecular interactions. Current studies are focused upon developing our understanding of reaction mechanisms in molecular crystals including bond-breaking and forming steps, and transport within the crystals.

## Experimental Section

**Crystal syntheses and gas–solid reactions:** All reagents were purchased from Aldrich, Lancaster, or Avocado and used as received. HCl gas was purchased from BOC (grade N2.6, 99.6% HCl;  $\text{H}_2\text{O}$  content < 10 ppm). Compound **1** was synthesized in quantitative yield as a green microcrystalline solid by combining methanolic solutions of  $\text{CuBr}_2$  and 3-bromopyridine. Exposure of **1** to vapors of concentrated aqueous HCl (32%) resulted in conversion to compound **2a** as a microcrystalline solid and was accompanied by a color change from green to brown (see Figure S1 in the Supporting Information). The reaction was allowed to occur over a period of 4 days to ensure completion. Exposure of **1** to dry HCl gas resulted in conversion to compound **2b** as a microcrystalline solid and was accompanied by a color change from green to brown within minutes (see Figure S2 in the Supporting Information). The reaction was allowed to continue for 3 days to ensure completion. Full details of syntheses and gas–solid reactions can be found in the Supporting Information.



X-ray powder diffraction: All polycrystalline samples were lightly ground in an agate mortar and pestle and placed in 0.7 mm glass capillaries. Diffraction data for **1** were collected on a Bruker-AXS D8 Advance powder diffractometer at room temperature using Cu K $\alpha$  radiation ( $\lambda = 1.54056 \text{ \AA}$ ). Measurements were made in the  $2\theta$  range  $3\text{--}30^\circ$  for indexing and structure solution, and in the  $2\theta$  range  $4\text{--}70^\circ$  for Rietveld refinement employing a variable count time (VCT) scheme.<sup>[21]</sup> The diffraction pattern was indexed using DICVOL91<sup>[22]</sup> to a monoclinic cell [ $F(19) = 56.1$ ,  $M(19) = 118.6$ ] and space group  $P2_1/c$  was assigned from volume considerations and a statistical consideration of the systematic absences. The datasets were background-subtracted for Pawley refinement<sup>[23]</sup> and for structure solution using the simulated annealing (SA) global optimization procedure, described previously,<sup>[24]</sup> that is now implemented in the DASH computer program.<sup>[25]</sup> The solved structure was refined against the  $4\text{--}70^\circ$  dataset using a restrained Rietveld method<sup>[26]</sup> as implemented in TOPAS,<sup>[27]</sup> with final  $R_{\text{wp}}$  of 0.0435,  $R_{\text{wp}}' = 0.0857$  (see Figure S3 in the Supporting Information). For **2a**, X-ray diffraction data were collected ( $3 \leq 2\theta \leq 75^\circ$ ; VCT) on a Bruker-AXS D8 Advance powder diffractometer at room temperature using Cu K $\alpha$  radiation. Following indexing and assignment of space group  $P1$ , Rietveld refinement was initiated using as a starting model the isostructural (3-BrpyH) $[\text{CuCl}_4]$ ,<sup>[11a]</sup> but enabling partial occupancy of both Cl and Br at all four halide ligand sites. Final occupancies of the four halide ligand sites obtained were Cl/Br: 67.4:32.6(7); 57.3:42.7(7); 54.6:45.4(7); 20.7:79.3(6), with final  $R_{\text{wp}}$  of 0.0409,  $R_{\text{wp}}' = 0.1175$  (see Figure S4 in the Supporting Information). For **2b**, X-ray diffraction data were collected ( $0 \leq 2\theta \leq 40^\circ$ ) at room temperature on beam line 1D31<sup>[28]</sup> at the European Synchrotron Radiation Facility (ESRF), Grenoble, France using  $\lambda = 0.93369(3) \text{ \AA}$ . A continuous scan mode ( $10^\circ \text{ min}^{-1}$  for 56 min) was employed and the capillary was translated to seven different positions (14 scans in total) to avoid sample degradation. Following indexing and assignment of space group  $P1$ , Rietveld refinement was initiated using **2a** as a starting model and enabling partial occupancy of both Cl and Br at all four halide ligand sites. A small amount of remaining **1** present required a two-phase mixed Rietveld–Pawley refinement to be conducted. This Pawley refinement of compound **1** was included to improve the overall fit to the pattern and enable more accurate determination of the occupancies of the halide sites in compound **2b**. Final occupancies of the four halide ligand sites obtained were Cl/Br: 67.3:32.7(5); 61.7:38.3(6); 57.7:42.3(5); 13.3:86.7(4), with final  $R_{\text{wp}}$  of 0.0837,  $R_{\text{wp}}' = 0.1482$  (see Figure S5). Powder diffraction studies are described in full detail in Supporting Information. CCDC 778567 (**1**), 778568 (**2a**), and 778569 (**2b**) contain the supplementary crystallographic data for this paper. These data can be obtained free of charge from The Cambridge Crystallographic Data Centre via [www.ccdc.cam.ac.uk/data\\_request/cif](http://www.ccdc.cam.ac.uk/data_request/cif).

Received: May 29, 2010

Published online: October 11, 2010

**Keywords:** crystal engineering · gas–solid reactions · halogen bonding · hydrogen bonding · supramolecular chemistry

- [1] a) G. J. Schmidt, *Pure Appl. Chem.* **1971**, 27, 647; b) L. R. MacGillivray, *CrystEngComm* **2002**, 4, 37; c) L. R. MacGillivray, G. S. Papaefstathiou, T. Frišćić, T. D. Hamilton, D.-K. Bučar, Q. Chu, D. B. Varshney, I. G. Georgiev, *Acc. Chem. Res.* **2008**, 41, 280; d) J. W. Lauher, F. W. Fowler, N. S. Goroff, *Acc. Chem. Res.* **2008**, 41, 1215.
- [2] a) *Organic Solid State Reactions, Topics in Current Chemistry Series*, Vol. 254, Springer, Berlin, **2005**; b) F. Toda, *CrystEngComm* **2002**, 4, 215; c) G. Kaupp, *CrystEngComm* **2003**, 5, 117.

- [3] a) A. W. Sun, J. L. Lauher, N. S. Goroff, *Science* **2006**, 312, 1030; b) X. Gao, T. Frišćić, L. R. MacGillivray, *Angew. Chem.* **2004**, 116, 234; *Angew. Chem. Int. Ed.* **2004**, 43, 232.
- [4] a) D. Fielder, D. H. Leung, R. G. Bergman, K. N. Raymond, *Acc. Chem. Res.* **2005**, 38, 351; b) M. Kawano, Y. Kobayashi, T. Ozeki, M. Fujita, *J. Am. Chem. Soc.* **2006**, 128, 6558.
- [5] a) Z. Wang, S. M. Cohen, *Chem. Soc. Rev.* **2009**, 38, 1315; b) J. S. Seo, D. Whang, H. Lee, S. I. Jun, J. Oh, Y. J. Jeon, K. Kim, *Nature* **2000**, 404, 982; c) M. J. Ingleson, J. Perez Barrio, J.-B. Guillaud, Y. Z. Khimyak, M. J. Rosseinsky, *Chem. Commun.* **2008**, 2680; d) Z. Wang, S. M. Cohen, *Angew. Chem.* **2008**, 120, 4777; *Angew. Chem. Int. Ed.* **2008**, 47, 4699; e) A. D. Burrows, C. D. Frost, M. F. Mahon, C. Richardson, *Angew. Chem.* **2008**, 120, 8610; *Angew. Chem. Int. Ed.* **2008**, 47, 8482; f) S. S. Kaye, J. R. Long, *J. Am. Chem. Soc.* **2008**, 130, 806.
- [6] a) C.-D. Wu, A. Hu, L. Zhang, W. Lin, *J. Am. Chem. Soc.* **2005**, 127, 806; C.-D. Wu, A. Hu, L. Zhang, W. Lin, *J. Am. Chem. Soc.* **2005**, 127, 8940; b) M. J. Ingleson, J. Perez Barrio, J. Basca, C. Dickinson, H. Park, M. J. Rosseinsky, *Chem. Commun.* **2008**, 1287; c) A. M. Shultz, O. K. Farha, J. T. Hupp, S. T. Nguyen, *J. Am. Chem. Soc.* **2009**, 131, 4204; d) T. Kawamichi, T. Haneda, M. Kawano, M. Fujita, *Nature* **2009**, 461, 633; e) K. Ohara, M. Kawano, Y. Inokuma, M. Fujita, *J. Am. Chem. Soc.* **2010**, 132, 30.
- [7] a) A. Lazuen Garay, A. Pichon, S. L. James, *Chem. Soc. Rev.* **2007**, 36, 846; b) W. Belcher, C. A. Longstaff, M. R. Neckenig, J. W. Steed, *Chem. Commun.* **2002**, 1602; c) D. Braga, M. Curzi, F. Grepioni, M. Polito, *Chem. Commun.* **2005**, 2915; d) C. J. Adams, M. A. Kurawa, M. Lusi, A. G. Orpen, *CrystEngComm* **2008**, 10, 1790; e) A. Pichon, S. L. James, *CrystEngComm* **2008**, 10, 1839; f) R. Kuroda, J. Yoshida, A. Nakamura, S.-i. Nishikiori, *CrystEngComm* **2009**, 11, 427; g) T. Frišćić, L. Fábán, *CrystEngComm* **2009**, 11, 743.
- [8] a) B. Rodríguez, A. Bruckmann, T. Rantanen, C. Bolm, *Adv. Synth. Catal.* **2007**, 349, 2213; b) B. Rodríguez, T. Rantanen, C. Bolm, *Angew. Chem.* **2006**, 118, 7078; *Angew. Chem. Int. Ed.* **2006**, 45, 6924; c) N. Giri, C. Bowen, J. S. Vyle, S. L. James, *Green Chem.* **2008**, 10, 627; d) W. C. Shearouse, D. C. Waddell, J. Mack, *Curr. Opin. Drug Discovery Dev.* **2009**, 12, 772.
- [9] a) S. J. Dalgarno, P. K. Thallapally, L. J. Barbour, J. L. Atwood, *Chem. Soc. Rev.* **2007**, 36, 236; b) J. Tian, P. K. Thallapally, S. J. Dalgarno, J. L. Atwood, *J. Am. Chem. Soc.* **2009**, 131, 13216; c) T. Tozawa, J. T. A. Jones, S. I. Swamy, S. Jiang, D. J. Adams, S. Shakespeare, R. Clowes, D. Bradshaw, T. Hasell, S. Y. Chong, C. Tang, S. Thompson, J. Parker, A. Trewin, J. Bacsa, A. M. Z. Slawin, A. I. Cooper, *Nat. Mater.* **2009**, 8, 973; d) P. Metrangolo, Y. Carcenac, M. Lahtinen, T. Pilati, K. Rissanen, A. Vij, G. Resnati, *Science* **2009**, 323, 1461.
- [10] a) M. Albrecht, M. Lutz, A. L. Spek, G. van Koten, *Nature* **2000**, 406, 970; b) D. Braga, G. Cojazzi, D. Emiliani, L. Miani, F. Grepioni, *Chem. Commun.* **2001**, 2272; c) C. J. Adams, H. M. Colquhoun, P. C. Crawford, M. Lusi, A. G. Orpen, *Angew. Chem.* **2007**, 119, 1142; *Angew. Chem. Int. Ed.* **2007**, 46, 1124; d) S. Supriya, S. K. Das, *J. Am. Chem. Soc.* **2007**, 129, 3464; e) A. Lennartson, M. Håkansson, S. Jagner, *New J. Chem.* **2007**, 31, 344.
- [11] a) G. Mínguez Espallargas, L. Brammer, J. van de Streek, K. Shankland, A. J. Florence, H. Adams, *J. Am. Chem. Soc.* **2006**, 128, 9584; b) G. Mínguez Espallargas, M. Hippler, A. J. Florence, P. Fernandes, J. van de Streek, M. Brunelli, W. I. F. David, K. Shankland, L. Brammer, *J. Am. Chem. Soc.* **2007**, 129, 15606; c) S. Libri, M. Mahler, G. Mínguez Espallargas, D. C. N. G. Singh, J. Soleimannejad, H. Adams, M. D. Burgard, N. P. Rath, M. Brunelli, L. Brammer, *Angew. Chem.* **2008**, 120, 1717; *Angew. Chem. Int. Ed.* **2008**, 47, 1693.
- [12] Excluding (traditional) inorganic solid-state materials such as silicates, zeolites, phosphonates, and metal chalcogenides.

- [13] G. Mínguez Espallargas in *Ideas in Chemistry and Molecular Sciences: Advances in Nanotechnology, Materials and Devices* (Ed.: Bruno Pignataro), Wiley-VCH, Weinheim, **2010**, pp. 115–138.
- [14] a) X.-Y. Wang, M. Scancella, S. C. Sevov, *Chem. Mater.* **2007**, *19*, 4506; b) R. Santra, K. Biradha, *CrystEngComm* **2008**, *10*, 1524; c) P. Dietzel, R. E. Johnson, R. Blom, H. Fjellvåg, *Chem. Eur. J.* **2008**, *14*, 2389.
- [15] a) L. Brammer, G. Mínguez Espallargas, S. Libri, *CrystEngComm* **2008**, *10*, 1712; b) F. Zordan, L. Brammer, P. Sherwood, *J. Am. Chem. Soc.* **2005**, *127*, 5979; c) F. Zordan, L. Brammer, *Cryst. Growth Des.* **2006**, *6*, 1374; d) L. Brammer, G. Mínguez Espallargas, H. Adams, *CrystEngComm* **2003**, *5*, 343.
- [16] Initial refinements provided populations of 1.889(7) Cl and 2.111(7) Br for **2a** and 2.037(6) Cl and 1.963(6) Br for **2b**. Since the populations are very close to 2.0 and the Br population cannot exceed the initial value of 2.0 (see **2a**), the final cycles of refinement were conducted with the overall constraint that populations of Cl and Br for each anion sum to 2.0.
- [17] L. Brammer, E. A. Bruton, P. Sherwood, *Cryst. Growth Des.* **2001**, *1*, 277.
- [18] G. Mínguez Espallargas, L. Brammer, P. Sherwood, *Angew. Chem.* **2006**, *118*, 449; *Angew. Chem. Int. Ed.* **2006**, *45*, 435.
- [19] a) Differences in (N–H···X) hydrogen-bond strengths for halide ions (X<sup>−</sup>) have been exploited, in part, to enable selective crystallization from aqueous solution of chloride, bromide, and iodide anions;<sup>[19b]</sup> b) R. Custelcean, T. J. Haverlock, B. A. Moyer, *Inorg. Chem.* **2006**, *45*, 6446.
- [20] O. P. Charkin, *J. Struct. Chem.* **1970**, *11*, 540 (translated from *Zhurnal Strukturnoi Khimii* **1970**, *11*, 574–576).
- [21] K. Shankland, W. I. F. David, D. S. Sivia, *J. Mater. Chem.* **1997**, *7*, 569.
- [22] A. Boulitf, D. Louër, *J. Appl. Crystallogr.* **1991**, *24*, 987.
- [23] G. S. Pawley, *J. Appl. Crystallogr.* **1981**, *14*, 357.
- [24] W. I. F. David, K. Shankland, N. Shankland, *Chem. Commun.* **1998**, 931.
- [25] W. I. F. David, K. Shankland, J. van de Streek, E. Pidcock, W. D. S. Motherwell, J. C. Cole, *J. Appl. Crystallogr.* **2006**, *39*, 910.
- [26] H. M. Rietveld, *J. Appl. Crystallogr.* **1969**, *2*, 65.
- [27] A. A. Coelho, *TOPAS-Academic*, version 3.1, **2004**; see <http://www.topas-academic.net>.
- [28] A. N. Fitch, *J. Res. Natl. Inst. Stand. Technol.* **2004**, *109*, 133.